Materials Research Proceedings 28 (2023) 937-942 https://doi.org/10.21741/9781644902479-102

Hot stamping of ultra-thin stainless steel for microchannels

GUO Nan[1,a], ZHANG Xianglu[1,b], HOU Zeran[1,c], YANG Daijun[2,d], MING Pingwen[2,e] and MIN Junying[1,f *]

[1]School of Mechanical Engineering, Tongji University, Shanghai 201804, China

[2]School of Automotive Studies, Tongji University, Shanghai 201804, China

[a]13guonan@tongji.edu.cn, [b]Xianglu_zhang@tongji.edu.cn, [c]zeranhou@tongji.edu.cn, [d]yangdaijun@tongji.edu.cn, [e]pwming@tongji.edu.cn, [f]junying.min@tongji.edu.cn

Keywords: Stainless Steel, Hot Stamping, Microchannel, Dimensional Accuracy

Abstract. Bipolar plate is one of the core components of a proton exchange membrane fuel cell (PEMFC), in which microchannels with regular distribution separate and distribute the fuel gas at the anode and oxygen/air at the cathode, and remove the reaction products from the cell. Dimensional deviations of microchannels affect assembly accuracy, thereby influencing the efficiency and performance of PEMFC. Ultra-thin stainless steel sheet is the most commonly used material for bipolar plate and stamping is an efficient way to form stainless steel microchannels. However, a challenge faced by the stamping process is how to improve the dimensional accuracy of stainless steel microchannels. Hereby we propose a hot stamping process of ultra-thin stainless steel sheet, which is of high potential to improve the dimensional accuracy of micro-channels. Uniaxial tensile tests are performed at room temperature (RT), 300, 600, and 900°C for an ultra-thin stainless steel 316L (SS316L). Results show that the strength of SS316L at 900 °C decreases significantly compared with that at RT, while the elongation is approximately 44%. Hot stamping process for stainless steel microchannels is developed, in which the ultra-thin sheet is heated by resistance heating. Stainless steel microchannels are hot stamped at 900°C, and the 3D profile and cross-sectional thickness distribution of which are measured. The measurement results show that the dimensional deviations of hot-stamped microchannels are lower than that of cold stamping, in terms of channel depth, rib width, and wall angle. Furthermore, the cross-sectional thickness distribution of the hot-stamped micro-channels has a similar trend as that of the cold stamping, and the thickness at the fillet is not significantly different (avg. + 1 μm) from that of the cold stamping.

Introduction

Fuel cell has a high-energy conversion efficiency of more than 40-50% [1], which is regarded as an ideal technology to utilize hydrogen energy. As the key component of a PEMFC, bipolar plates (BPPs) with fine microchannel features play the role of separating and distributing hydrogen and oxygen/air, providing mechanical support to the fuel cell stack, collecting, and conducting current, etc. Dimensional deviations of microchannel features affect assembly accuracy, thereby influencing the efficiency and performance of PEMFC. With the advantage of high electrical conductivity and mechanical strength as well as low cost, stainless steel is widely utilized to fabricate BPPs, and the stamping process is one of the most used methods to manufacture stainless steel BPPs due to its relatively high productivity and low cost. However, dimensional errors are unavoidable on stainless steel BPPs due to the characteristics of residual stress and springback in stamping process, which contributes to uneven pressure distribution, larger contact resistance, and higher GDL porosity [2]. It is reported that fabricating BPPs with fine flow microchannel features, i.e., flow channels with a channel width, a rib width, and a pitch length of 0.5, 0.5, and 1.5 mm, respectively, is a challenge for the current stamping process [3]. Thus, several advanced forming

processes have been developed in the literature to increase the dimensional accuracy and the ultimate flow channel features of BPPs. Based on ultra-thin ferritic stainless steel sheets with thickness of 100 and 75 μm, Bong et al. [4] conducted a two-step stamping process to fabricate microchannels, they found that the two-step forming process evidently increase the forming depth and precision of ferritic stainless steel microchannels. Xu et al. [5] revealed that the depth limit of titanium microchannels is increased from 438.1 μm in single-step forming process to 621.1 μm in three-step forming process. Since increasing forming temperature can reduce the strength of materials, thus reducing residual stress and springback and improving the forming accuracy of parts, some heat-assisted forming processes have been proposed for microchannels. By conducting warm stamping process at the temperature up to 300°C, Lakshmi [6] improved the formability of ferritic stainless steel microchannels. Moreover, they found that increasing forming temperature can reduce the springback of microchannels.

In this work, uniaxial tensile tests were performed at room temperature (RT), 300, 600, and 900°C for an ultra-thin stainless steel SS316L. The variation of strength and elongation of ultra-thin SS316L to temperature was discussed to evaluate the properly forming temperature of ultra-thin SS316L. Then a lab-scale hot stamping platform with an on-site resistance heating device was built to verify the hot stamping process of ultra-thin SS316L microchannels. Channel depth, rib width, and wall angle were measured to characterize the dimensional accuracy of ultra-thin SS316L microchannels under hot stamping process.

Experiments

Uniaxial Tensile Test. An ultra-thin austenitic stainless steel SS316L with a thickness of 100 μm was used in this study. Uniaxial tensile tests were performed to obtain the mechanical properties of ultra-thin SS316L at elevated temperatures. Fig. 1a shows the high-temperature uniaxial tensile testing system with a muffle furnace and digital image correlation technic (DIC). The DIC cameras equipped with blue light bandpass filters record the deformation of the specimen through a glass window on the furnace to calculate strain fields. Additionally, two blue LED lights with a wavelength of 450 nm were used to illuminate the specimen from different directions to ensure sufficient image contrast. The geometric dimension of the uniaxial tensile specimen is shown in Fig. 1b according to the ISO 6892-2 standard. All specimens were cut off along the rolling direction by electrical discharge machining to ensure high edge quality. The test temperature of SS316L includes room temperature (RT), 300, 600, and 900°C, and three samples were tested at each temperature to ensure reproducibility.

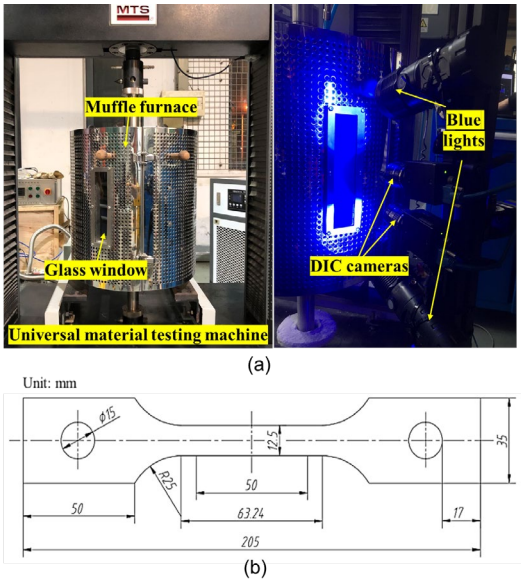

Fig. 1. (a) The high-temperature uniaxial tensile testing system and (b) the geometric dimension of the uniaxial tensile specimen.

Microchannel Hot Stamping Test. The microchannel structure is shown in Fig. 2a, and the cross-sectional geometry of the stamping tool is shown in Fig. 2b, where the dimensions of the channel width, rib width, channel depth, wall angle, and corner radius are also depicted. Fig. 2c illustrates a lab-scale hot stamping platform built in this study, where a pair of electrode clamps is embedded into the system to heat the ultra-thin SS316L sheet by resistance heating. An automatic

tensioning device composed of compression springs and linear guides is assembled to the clamp to prevent ultra-thin SS316L sheet buckling caused by constrained thermal expansion. During the hot stamping process, the initial distance between the upper and lower tool was 150 mm. The ultra-thin SS316L sheet started to be heated by resistance heating with a power of 22.5 kW at 0 s, and the upper tool started to move downward with a velocity of 140 mm/s at 5 s. The ultra-thin SS316L sheet was heated to the target temperature at 6 s, and meanwhile, the upper tool was down to a distance of 10 mm from the lower tool. Then the power was off and the upper and lower tools were closed at 6.1 s. Then the formed microchannel sample was cooled in the tool from 6.1 s to 7 s. Moreover, a solid lubricant boron nitride (BN) was applied to reduce the friction coefficient between the ultra-thin SS316L sheet and tool.

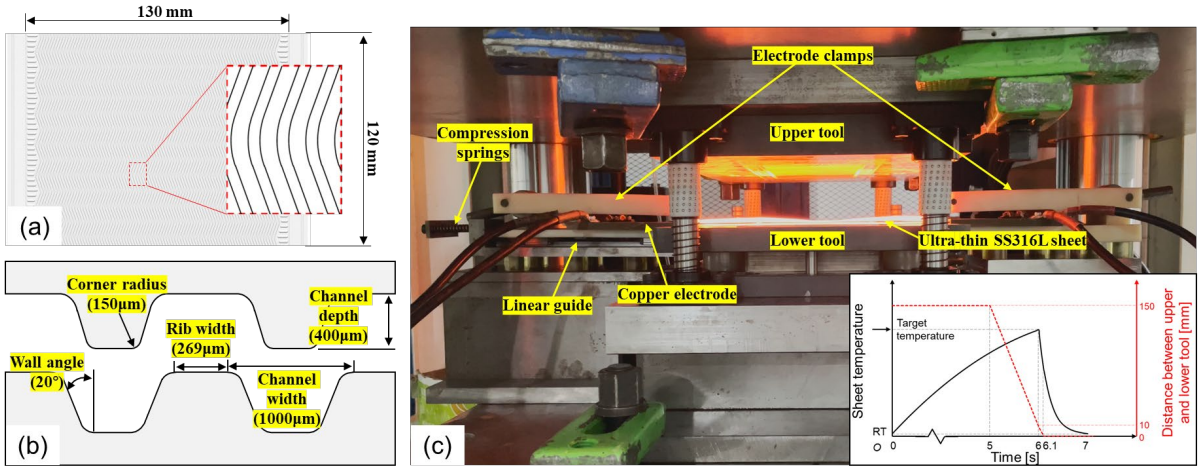

Fig. 2. (a) The designed microchannel structure, (b) the cross-sectional geometry of the stamping tool, and (c) an illustration of the microchannel hot stamping process.

Geometrical and Thickness Measurements. The surface topographies of formed microchannels were measured by a non-contact 3D optical profilometer KEYENCE VR-5000, through which channel width, rib width, and wall angle of the formed microchannels were extracted. Cross-sectional samples were cut along the direction perpendicular to the channels by laser cutting and mounted with resin at room temperature. Then the samples were polished with 800, 1500, and 2500 Grit sandpapers in sequence and observed with an optical microscope to evaluate the thickness of the microchannels.

Results and Discussion

The engineering stress-strain curves of ultra-thin SS316L at different temperatures are shown in Fig. 3a. In the temperature range from RT to 600°C, although the flow stress decreases with the increase of temperature, it can be seen from the stress-strain curves that strain hardening is the dominant. At 900°C, the stress-strain curve of ultra-thin SS316L is more significantly affected by temperature softening, and the strength is reduced to 104 MPa. Fig. 3b represents the variation of ultimate tensile strength and elongation of ultra-thin SS316L with temperature. The ultimate tensile strength (UTS) of ultra-thin SS316L decreases from 620 MPa at room temperature to 104 MPa at 900°C; however, the elongation decreased significantly from room temperature to 600°C, with a minimum value of 26% at 600°C, and with the temperature increasing up to 900°C, the elongation increased to 44%. This indicates that increasing the forming temperature can reduce the strength of the ultra-thin SS316L, thus potentially reduce residual stress and springback to improve the forming accuracy of parts. However, a temperature range, namely 300–600°C, should

be avoided in developing warm/hot stamping process for ultra-thin SS316L, because the elongation of which is much lower than that at room temperature.

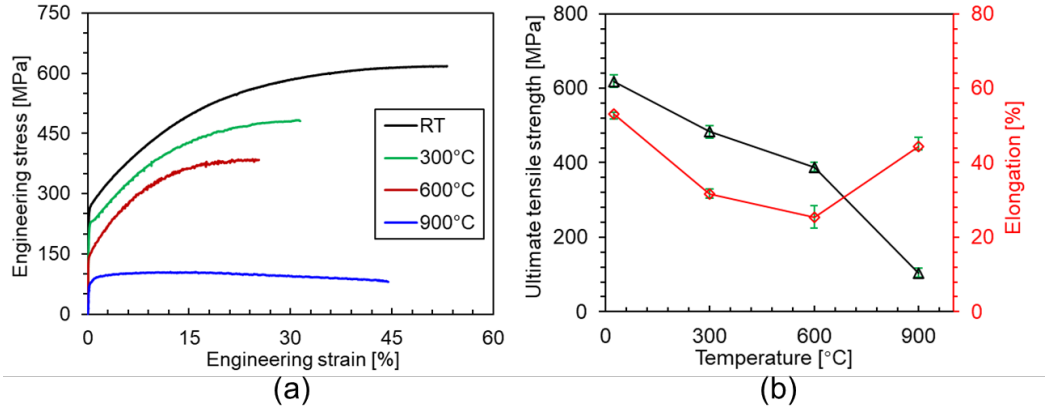

Fig. 3. (a) Engineering stress-strain curves of ultra-thin SS316L at different temperatures and (b) variation of UTS and elongation of ultra-thin SS316L with temperature.

The microchannel features of BPP have significant effects on the distribution of reaction gas, heat and water management, mechanical stability, and consequently on the performance, reliability, and durability of fuel cells [7]. The rib width (a) determines the contact area between the BPP and the MEA, a narrower rib width means a smaller contact area, and a larger contact resistance between the BPP and MEA as well as reduced PEMFC performance. The channel depth (c) and wall angle (β) mainly affect the mass transfer towards MEA and production water removal ability, and a deeper channel depth and a smaller wall angle enhance electrochemical reaction rate and fuel efficiency. Fig. 4 shows a microchannel sample hot-stamped at 900°C, where measurement of microchannel features was conducted within the red dashed wireframe.

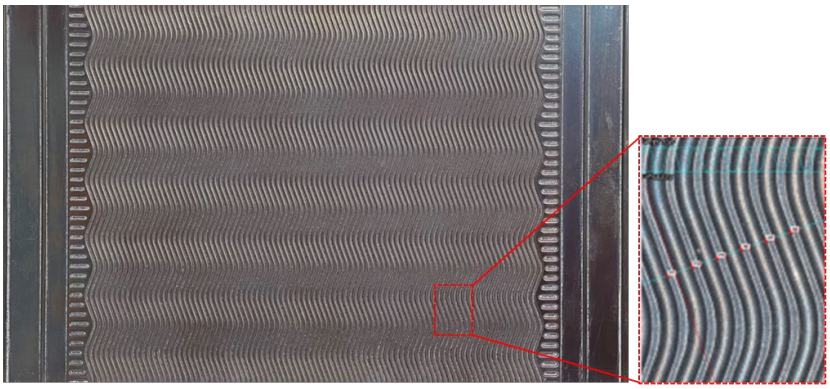

Fig. 4. Hot-stamped microchannel sample.

Measurement results of the microchannel features formed via hot stamping and cold stamping are shown in Fig. 5a. Average c of the hot-stamped microchannel is 394.2 μm, which is closer to the design value (400 μm) compared to that of the cold-stamped microchannel. For a and β, the values of hot-stamped sample are smaller than those of cold-stamped sample, which benefits from the reduced springback under hot stamping process. The dimensional deviations of c, a, and β of the cold-stamped microchannel are larger than that of hot-stamped microchannel. The large dimensional deviations are caused by highly localized stamping force [8]. This indicates that the

hot stamping process improves the dimensional accuracy of ultra-thin SS316L microchannels. Fig. 5b represents the thickness distribution of hot-stamped and cold-stamped microchannels, which have a similar trend, i.e., positions 1, 5, and 9 exhibit a larger thickness, and the maximum thinning appears at the fillet where the sheet metal contacts the lower tool (position 2). There is no significant difference between the minimum thicknesses of the hot-stamped and cold-stamped microchannels (average difference at position 2 is 1 μm).

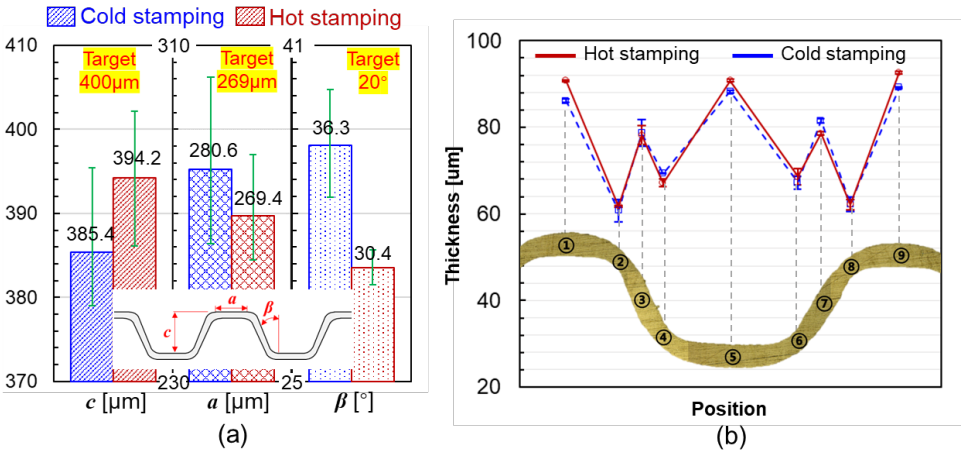

Fig. 5. (a) Comparison of channel depth (c), rib width (a), and wall angle (β) between hot stamping and cold stamping microchannels and (b) cross-sectional thickness distribution of microchannels via hot stamping and cold stamping.

Summary

In this work, the variation of strength and elongation of ultra-thin SS316L at elevated temperatures were investigated by applying high-temperature uniaxial tensile tests. In order to verify the hot stamping process of ultra-thin SS316L microchannels, a lab-scale hot stamping platform with an on-site resistance heating device was built. The dimensional accuracy of hot-stamped ultra-thin SS316L microchannels was characterized, and conclusions can be drawn here:

1) 900°C might be the appropriate hot stamping temperature for ultra-thin SS316L microchannels because of the relative low strength of 104 MPa and an elongation of about 44% of ultra-thin SS316L at 900°C;
2) Compared to cold stamping, hot stamping at 900°C increase the dimensional accuracy of ultra-thin SS316L microchannels in terms of channel depth (from 385.4 μm to 394.2 μm with a target of 400 μm), rib width (from 280.6 μm to 269.4 μm with a target of 269 μm), and wall angle (from 36.3° to 30.4° with a target of 20°).

Acknowledgments

The authors would like to acknowledge the financial support for this research provided through the National Key Research and Development Program of China (No. 2020YFB1505900).

References

[1] K. Sopian, W.R.W. Daud, Challenges and future developments in proton exchange membrane fuel cells, Renewable energy 31(2006) 719-727. https://doi.org/10.1016/j.renene.2005.09.003
[2] L. Peng, Y. Wan, D. Qiu, P. Yi, X. Lai, Dimensional tolerance analysis of proton exchange membrane fuel cells with metallic bipolar plates, J. Power Source. 481 (2021). https://dx.doi.org/10.1016/j.jpowsour.2020.228927
[3] Y. Leng, P. Ming, D. Yang, C. Zhang, Stainless steel bipolar plates for proton exchange membrane fuel cells: Materials, flow channel design and forming processes, J. Power Source. 451 (2020). https://dx.doi.org/10.1016/j.jpowsour.2020.227783

[4] H.J. Bong, J. Lee, J.H. Kim, F. Barlat, M.G Lee, Two-stage forming approach for manufacturing ferritic stainless steel bipolar plates in PEM fuel cell: Experiments and numerical simulations, Int. J. Hydrogen Energ. 42 (2017) 6965-6977. https://dx.doi.org/10.1016/j.ijhydene.2016.12.094
[5] Z. Xu, Z. Li, R. Zhang, T. Jiang, L. Peng, Fabrication of micro channels for titanium PEMFC bipolar plates by multistage forming process, Int. J. Hydrogen Energ. 46 (2021) 11092-110103. https://dx.doi.org/10.1016/j.ijhydene.2020.07.230
[6] R.N. Lakshmi, Forming of ferritic stainless steel bipolar plates, Electronic Theses and Dissertations, 205 (2012). https://scholar.uwindsor.ca/etd/205
[7] J. Wang, Theory and practice of flow field designs for fuel cell scaling-up: A critical review, Appl. Energ. 157 (2015) 640-663. https://doi.org/10.1016/j.apenergy.2015.01.032
[8] C. Turan, Ö.N. Cora, M. Koç, Effect of manufacturing processes on contact resistance characteristics of metallic bipolar plates in PEM fuel cells, Int. J. Hydrogen Energ. 36 (2011) 12370-12380. https://doi.org/10.1016/j.ijhydene.2011.06.091